Applied Nanoscience (2020) 10:2813–2825
https://doi.org/10.1007/s13204-019-01087-1

ORIGINAL ARTICLE

Functionalization of the magnetite nanoparticles with polysilsesquioxane-bearing N- and S-complexing groups to create solid-phase adsorbents

Inna V. Melnyk[1,2] · Nataliya V. Stolyarchuk[2] · Veronika V. Tomina[2] · Oleksandr V. Bespalko[2] · Miroslava Vaclavikova[1]

Received: 17 December 2018 / Accepted: 10 June 2019 / Published online: 26 June 2019

Abstract
Sol–gel method based on the reaction of hydrolytic co-polycondensation of alkoxysilanes was applied to obtain composites of magnetite and silica with amino and mercapto functional groups of core–shell structure. Magnetite core ensures easy removal of materials from solutions in a quick and effective way with a help of a magnet. Using 1,2-bis(triethoxysilyl)ethane as a structure-forming agent (instead of traditional tetraethoxysilane) allowed synthesis of mesoporous samples with well-developed porous structure (specific surface area values of 400–800 m^2/g). In combination with high content of available functional groups, introduced to the process of one-pot synthesis using 3-aminopropyltriethoxysilane and 3-mercaptopropyltriethoxysilane as functionalyzing agents, it endowed the synthesized composites with high sorption capacities to silver(I), copper(II), and lead(II) ions. Meanwhile, the affinity to the molecules of dyes (Acid Red 88 and Methylene Blue) was shown to be in direct correlation with the composites' surface charges and uptake can reach 118 mg/g and 88 mg/g, respectively. These results indicate the possibility of magnetite nanoparticles' one-step functionalization with mesoporous silica layers and simultaneous introduction of different functional groups. Such properties make them very attractive for application in adsorption technologies as effective adsorbents of metal ions as well as organic pollutants.

Keywords Magnetite particles · Mesoporous shell · Amino groups · Mercapto groups · Ag(I), Pb(II), and Cu(II) ions adsorption · Organic dyes

Introduction

Last 15 years, magnetic nanoparticles have been widely used in medicine (Thanh 2012), catalysis (Zhang et al. 2011), biotechnology (Pogorilyi et al. 2014a, b JMCB), and sorption processes (Goncharuk et al. 2003; Turanska et al. 2012; Xin et al. 2012).

A number of European cities are facing an unfavorable environmental situation due to the presence of metallurgical enterprises (ferrous and nonferrous metals), thermal power plants, petrochemical, cement and slate plants, and electroplating workshops. A feature of such industries is the formation of significant amount of sewage containing heavy metal ions which are harmful to the environment and their release needs to be eliminated. Thus, modern effective, safe, and inexpensive methods of removing and disinfecting pollutants are of current interest. One of the approaches removing heavy metals from aqueous solutions is the use of magnetic composites based on magnetite nanoparticles (Goncharuk et al. 2003; Turanska et al. 2012). There are several advantages of using such objects: (1) it allows selective removal of the target components and (2) it facilitates the separation of sorbents with bound adsorbate from the solution due to the use of a magnet, which cannot be achieved using sorbents without the magnetically sensitive core. A few research articles describe the removal of Cu (Wang et al. 2010; Chung et al. 2012; Ozmen et al. 2010; Kusyak et al. 2011; Huang and Hu 2008), Pb (Wang et al. 2010; Chung et al. 2012; Kusyak et al. 2011; Izanloo et al. 2019; Tang et al. 2013; Tan et al. 2012; Huang and Hu 2008; Li et al. 2011; Wang et al. 2015), Cd (Wang et al. 2010; Kusyak et al.

✉ Inna V. Melnyk
in.melnyk@gmail.com

[1] Institute of Geotechnics Slovak Academy of Sciences, 45, Watsonova Str, Kosice 04001, Slovak Republic

[2] Chuiko Institute of Surface Chemistry of National Academy of Sciences of Ukraine, 17, General Naumov Str, Kyiv 03164, Ukraine

2011; Tang et al. 2013; Huang and Hu 2008), Hg (Huang and Hu 2008; Li et al. 2011; Hakami et al. 2012; Zhang et al. 2013; Dong et al. 2008) using magneto sensitive adsorbents with polysiloxane layer containing functional groups.

In general, procedures of the functionalization of magnetite particles involved two stages. The first stage implied preparation of Fe_3O_4@SiO_2 particles, e.g., by loading mesoporous silica with magnetic particles (Kim et al. 2003; Chung et al. 2012), coating Fe_3O_4 using TEOS in ethanol/water solution with ammonium hydroxide as catalyst at pH 9.5 (Tang et al. 2013; Izanloo et al. 2019; Li et al. 2013), using TEOS in water/glycerol solution with acetic acid at pH 4.6 (Huang and Hu 2008), coating Fe_3O_4 nanoparticles using sodium silicate solution at pH 6 (Wang et al. 2010; Zhang et al. 2013), and applying mesoporous coating using TEOS (Hakami et al. 2012; Wang et al. 2015). The second stage involves subsequent grafting of Fe_3O_4@SiO_2 using organosilanes with functional groups: amino-silanes APTMS (Wang et al. 2010; Chung et al. 2012; Tang et al. 2013), APTES (Wang et al. 2015; Li et al. 2013), N-[3-(trimethoxysilyl) propyl] ethylenediamine (Chung et al. 2012), N1-(3-trimethoxysilylpropyl) diethylenetriamine (Chung et al. 2012) to introduce amino groups; mercapto-silanes MPTES (Kim et al. 2003) or MPTMS (Huang and Hu 2008; Hakami et al. 2012; Zhang et al. 2013) to introduce thiol groups. Izanloo et al. (2019) simultaneously used APTMS and MPTMS for grafting both amino and thiol groups on the adsorbent surface.

There were attempts to conduct one-pot synthesis to introduce thiol groups by modified Stober method via adding TEOS with MPTMS in one stage (Li et al. 2011); however, the procedure involved adding CTAB for structure formation and its subsequent removal. Ozmen et al. (2010) as well as Kusyak et al. (2011) suggested grafting Fe_3O_4 with APTES without other structure-forming agents, but such technique could lead to great concentration of amino groups on surface and their unavailability for adsorption of heavy metals. It is known that porous materials have large sorption capacity and volume, but their synthesis via template method is time-consuming (multi-stage) and cost inefficient (due to necessity of using template and its subsequent removal and utilization). The advantages of magnetic particles have already been mentioned above. Therefore, the aim was to synthesize composites in the form of spherical particles with a magnetite nucleus (sensitive to magnetic field) and a shell of mesoporous silica with functional groups: (1) using one-pot synthesis; (2) making porous samples with well-developed surface; (3) avoiding additional structure-forming agents that require washing; (4) saving the possibility of introducing several types of groups simultaneously; (5) avoiding 'overloading' with groups by increasing space between them; and (6) creating additional sites for adsorption of organic molecules via hydrophobic interactions.

As mentioned above, the sol–gel method based on the reaction of hydrolytic polycondensation of alkoxysilanes, which is particularly suitable for the synthesis of organo-inorganic hybrid silica materials, was chosen for magnetite functionalization (Zub et al. 2005; Dabrowski et al. 2005; Trofimchuk et al. 2006; Zub et al. 2008). Several studies on functionalization of magnetite with polysiloxane layers containing amino (Mel'nik et al. 2012; Melnyk and Zub 2012; Pogorilyi et al. 2013; Zavoiura et al. 2015; Melnyk et al. 2016; Gdula et al. 2017) and mercapto groups (Pogorilyi et al. 2014a, b JMCB; Stolyarchuk et al. 2018; Melnyk et al. 2018) via one-pot synthesis were performed by our team. However, specific surface area of such composites with amino functional groups was 100–140 m^2/g and mercapto 33–125 m^2/g. The dilution of mercapto groups with methyl or propyl functions could increase surface area to 360 and 290 m^2/g due to the formation of smaller particles (Melnyk et al. 2018), however, for amino-functionalized samples light increase in specific surface to 180 m^2/g was observed with incorporation of additional methyl groups (Pogorilyi et al. 2013). In this study, we aimed to increase the specific surface area of the materials covering magnetite with porous coating. Two functional groups ≡$Si(CH_2)_3NH_2$ and ≡$Si(CH_2)_3SH$, and their combinations were introduced into the surface layer using trifunctional silanes APTES and MPTMS. The mesoporosity of the samples derived from structuring silane with ethylene bridge between silicon atoms. The adsorption properties of synthesized materials with respect to copper(II), silver(I), lead(II) ions, and some dyes were examined and compared.

Materials and methods

Chemicals and reagents

The following compounds were used for the Fe_3O_4 synthesis: iron(II) chloride, $FeCl_2$•$4H_2O$ (Sigma-Aldrich, 99%); iron(III) chloride, $FeCl_3$•$6H_2O$ (Sigma-Aldrich, 98%); and ammonium hydroxide, NH_4OH (Aldrich, 25% aqueous solution).

Compounds used for functionalization of magnetite nanoparticles: 1,2-bis(triethoxysilyl)ethane, $(C_2H_5O)_3Si(CH_2)_2Si(OC_2H_5)$ (BTESE, 95%, Fluorochem) as a structure-forming agent; 3-mercaptopropyltrimethoxysilane, $(CH_3O)_3Si(CH_2)_2SH$ (MPTMS, 95%, Aldrich) as a source of mercapto groups; 3-aminopropyltriethoxysilane, $(C_2H_5O)_3Si(CH_2)_3NH_2$ (APTES, Aldrich, 99%) as a source of amino groups; NH_4F (analytical grade, Reahim, Ukraine) as a catalyst; and ethanol (96%, PJSC "Oxygen Plant").

Reagents which were used in sorption studies: silver(I) nitrate, $AgNO_3$ (pure p.a., microCHEM, Slovakia), lead(II) nitrate, and $Pb(NO_3)_2$ (pure p.a., Lachema a.s., Czech

Republic); copper(II) nitrate, $Cu(NO_3)_2 \bullet 3H_2O$ (analytical grade, ITES Vranov, Slovakia); sodium nitrate, $NaNO_3$ (anal. grade, ITES Vranov, Slovakia); Methylene Blue, $C_{16}H_{18}ClN_3S$ (MB, 95%, microCHEM); and Acid Red 88, $C_{20}H_{13}N_2NaO_4S$ (AR, Glentham life science, UK). All reagents were used as received, without further purification.

Syntheses of magnetite particles

The magnetite nanoparticles were obtained by co-precipitation of iron(II) and (III) salts in an ammonium medium (Wang et al. 2010; Mel'nik et al. 2012). Briefly, iron(II) chloride (4.3 g) and iron(III) chloride (11.8 g) (in molar ratio: $Fe^{2+}/Fe^{3+}=1/2$) were dissolved in 250 ml of distilled water at 80 °C, under nitrogen flow. Next, 25 ml of ammonia solution was slowly added to the mixture. The black magnetite precipitate was produced within few seconds, and kept under 80 °C and mechanical stirring, during 30 min. After this time, the heating was switched off and samples were cooled down to room temperature. The magnetic nanoparticles were separated from solution by decantation using permanent neodymium magnet. To remove residual solvents, the magnetite particles were cleaned by repeated cycles of water and ethanol. After washing the magnetite, ethyl alcohol was added and the formed suspension was stored for further functionalization.

Techniques for functionalizing magnetite particles

To avoid magnetite aggregates, the 15 min sonication was employed to the magnetite–ethanol suspension.

Magnetite functionalization with amino groups Fe_3O_4@BA

For **Fe_3O_4@BA4** sample, 0.52 ml of BTESE were mixed with 2.5 ml of ethanol (for the synthesis of **Fe_3O_4@BA8**, 1.04 ml of BTESE were dissolved in 5 ml of ethanol). Then, 2.5 ml of magnetite suspension (50 mg of magnetite) were transferred to a round-bottom flask with a mechanical stirrer, followed by the addition of BTESE solution and 0.3 ml of 1% aqueous NH_4F (0.6 ml for **Fe_3O_4@BA8**). The previous hydrolysis of bissilane lasted 1 h at a stirring rate of ≈ 100 rpm. After preliminary hydrolysis, the solution of 0.1 ml APTES was added in 2.5 ml of ethanol. The reaction continued for 2 h under constant stirring.

Magnetite functionalization with mercapto groups Fe_3O_4@BM

For **Fe_3O_4@BM4** sample, 2.1 ml of BTESE were dissolved in 10 ml of ethanol (while for **Fe_3O_4@BM8** preparation, 1.04 ml of BTESE and 5 ml of ethanol were used). Then, 10 ml of magnetite suspension (200 mg of magnetite) were transferred to a round-bottom flask with a mechanical stirrer followed by the addition of BTESE–ethanol solution and 1.2 ml of 1% aqueous NH_4F (0.6 ml for **Fe_3O_4@BM8**). The previous hydrolysis of bissilane lasted 1 h with at constant stirring ≈ 100 rpm. After preliminary hydrolysis, 0.24 ml of MPTMS solution was added into 10 ml of ethanol (0.06 ml MPTMS and 2.5 ml of ethanol were used for **Fe_3O_4@BM8**). The reaction continued for 2 h under constant stirring and temperature 30 °C maintained by water bath.

Magnetite functionalization with amino and mercapto groups Fe_3O_4@BAM

To prepare **Fe_3O_4@BAM4** sample, 1.04 ml of BTESE were dissolved in 5 ml of ethanol. Then, 2.5 ml of magnetite suspension (50 mg of magnetite) were placed in a round-bottom flask with a mechanical stirrer followed by the addition of BTESE solution and 0.6 ml of 1% aqueous NH_4F. The previous hydrolysis of bissilane lasted for 1 h at a stirring rate ≈ 100 rpm. Afterwards, 0.08 ml of APTES solution was added in 2.5 ml of ethanol and 0.12 ml of MPTMS in 2.5 ml of ethanol (0.04 ml APTES in 1.3 ml of ethanol and 0.06 ml MPTMS in 1.3 ml of ethanol were used for **Fe_3O_4@BAM8**). The reaction continued for 2 h under constant stirring.

When the reactions finished, the external magnetic field (permanent magnet) was applied to separate nanoparticles from residual supernatant. Modified magnetite samples were washed with ethanol (3 × 20 ml) and dried at 80 °C for 24 h. Yields are summarized in Table 1.

Characterization

The CHNS analysis was performed by elementary analyzer Vario MACRO cube (Elementar Analysensysteme GmbH, Germany) using thermal conductivity detector.

The zeta potential was measured using a Zetasizer Nano ZS (Malvern, Great Britain) with 2 g/l sample concentration and 1 mmol/l $NaNO_3$.

The morphology of nanoparticles was characterized with the Analytical Scanning Electron Microscope JEOL JSM-6060 LA. To prevent the accumulation of surface charge and to increase the image contrast, the samples were covered with the shell of gold by cathode sputtering (JEOL Fine Coat, Ion Sputter JFC-1100).

Photon cross-correlation spectroscopy (PCCS) analysis was conducted on a Nanophox particle size analyzer (Sympatec, Germany). A portion of aqueous suspension of each sample (prepared using US bath) was diluted with the stabilizer to achieve a suitable concentration for measurement. The measurements were repeated three times for each sample.

DRIFT spectra were recorded on a Thermo Nicolet Nexus FTIR spectrometer in the 400–4000 cm^{-1} range, with a

Table 1 Composition and some characteristics of the samples

Sample	BTESE/APTES/MPTMS	Funct. groups – NH_2/–SH (mmol/g)	Yield (%)	S_{sp} (m^2/g)	V_s (cm^3/g)	d_{aver}, pore (nm)	d_{part} (nm), XRD data	S (%)	N (%)	H (%)	C (%)	ζ-potent (mV)
Fe_3O_4@BA4	4/1/0	2.82/0	40	408	0.64	6.3	24.4	0	3.8	3.5	15.8	29.44
Fe_3O_4@BA8	8/1/0	0.87/0	44	750	0.70	3.7	35.3	0	1.2	4.3	16.0	26.04
Fe_3O_4@BM4	4/0/1	0/0.93	73	575	0.43	3.7	16.8	2.9	0	3.8	14.8	−27.03
Fe_3O_4@BM8	8/0/1	0/0.61	53	520	0.33	3.7	25.6	1.9	0	4.6	14.9	−32.22
Fe_3O_4@BAM4	4/0.5/0.5	0.70/1.00	52	631	0.53	3.4	22.1	3.1	1.0	4.3	18.0	4.01
Fe_3O_4@BAM8	8/0.5/0.5	0.50/0.76	72	818	0.59	2.9	23.4	2.4	0.7	4.4	18.3	21.64

resolution of 8 cm^{-1}. The samples were ground with KBr at the weight ratios of sample:KBr = 1:30.

The low-temperature nitrogen adsorption–desorption isotherms were recorded with a Kelvin-1042 instrument at − 196 °C (Costech Microanalytical). Prior the measurements, the samples were degassed at 100 °C for 3 h, in the helium atmosphere. The BET specific surface area was examined in the 0.03–0.35 range of relative pressures, the pore size using BJH.

X-ray powder-diffraction (XRD) patterns of synthesized nanoparticles were collected by use of a Rigaku SmartLab® X-ray diffractometer equipped with a CuKα source ($\lambda = 1.54056$ Å). The data were collected in the 2θ range from 10° to 80° with a step of 0.05° and exposition time of 50 s per step.

For Ag^+, Pb^{2+}, and Cu^{2+} adsorption study, a specimen ($m = 0.01 \pm 0.0005$ g) was introduced in contact with metal ion aqueous solution [V = 10 ml, pH (Ag^+) ~ 2.0, pH (Pb^{2+}) ~ 4.2, pH (Cu^{2+}) ~ 5.0] for 24 h at 25 °C. The ionic strength was adjusted by the preparation of the metal solutions using the 0.1 M solution of $NaNO_3$. The concentration of silver(I), lead(II), and copper(II) ions in the solution before and after sorption was determined by Atomic absorption spectrometer Varian AA 240 FS.

Similar batch-type procedure (static mode) was carried out for the study of dyes adsorption. Batches of samples (0.01 g) were poured with 10 ml of dyes solutions (with concentration 1 mmol/l) at pH ~ 7.0, constant temperature 25 °C, and contact time 24 h. The concentration of dyes was determined by a Helios Gamma UV–Vis spectrophotometer (Thermo Electron Corporation, UK) by measuring the dyes absorbance at 664 nm (MB) and 505 nm (AR).

Results and discussion

Sol–gel method based on the reaction of hydrolytic co-polycondensation of BTESE as a structure-forming agent and MPTMS and APTES as functionalizing agents was used to functionalize magnetite particles with polysilsesquioxane layers containing amino (**Fe_3O_4@BA**), mercapto (**Fe_3O_4@BM**), and a combination of amino and mercapto functional groups (**Fe_3O_4@BAM**). The synthesis was conducted in single stage, as schematically depicted in Fig. 1. As it was shown previously for Fe_3O_4 functionalized with TEOS, the stability of the particles in the acidic medium [important for the regeneration of the particles (Wang et al. 2010)] is determined by Si:Fe ratio (Pogorilyi et al. 2014a, b RSCA). Therefore, in the syntheses with BTESE, the similar molar ratio between Fe and Si (1:20) was kept, which provided the stability of obtained materials in an acidic environment (Melnyk et al. 2018).

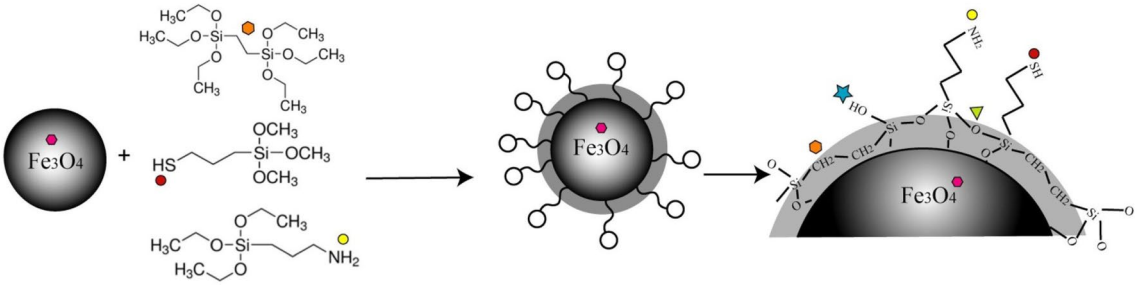

Fig. 1 Sol–gel one-stage functionalisation of magnetite nanoparticles

Another peculiarity of the synthesis with BTESE is that it requires preliminary hydrolysis, but the excess water promotes precipitation of bissilane (Stolyarchuk et al. 2018). Therefore, in our synthesis approach, BTESE–ethanol solution was mixed with magnetite–ethanol suspension to form primary globules on the surface of magnetite particles, catalyzed with fluoride ions (Stolyarchuk et al. 2016, 2018). To avoid the precipitation of bissilane, the hydrolysis was conducted due to the water from an aqueous solution of the catalyst, and no additional water was added (Stolyarchuk et al. 2018). In addition, only afterwards, ethanol solutions of functionalizing silanes were added to ensure the location of functional groups on the surface.

The characteristics on the samples that we synthesized are presented in Table 1.

Analysing the content of functional groups in samples **Fe_3O_4@BA8** (−NH_2, 0.87 mmol/g), **Fe_3O_4@BM8** (−SH, 0.61 mmol/g), and **Fe_3O_4@BAM4** (−NH_2/−SH, 0.7 vs 1.0 mmol/g) given in Table 1, it is possible to conclude that the presence of APTES improves the hydrolysis/polycondensation of MPTMS due to the formation of partially alkaline medium by amino groups. However, in the presence of MPTMS in the reaction medium, the hydrolysis/polycondensation of the APTES itself is worse than during the synthesis of a monofunctional sample. Nevertheless, incorporated in the surface layer of polysiloxane xerogels along with 3-aminopropyl groups, 3-mercaptopropyl groups were shown to behave in an "inert" fashion (Zub et al. 2008), and similar behavior of the same groups is expected in the surface layer of bifunctional magnetite composites, **Fe_3O_4@BAM**.

According to SEM images presented in Fig. 2, the functionalized composites are highly dispersed. Individual particles are spherical and agglomerate to form a monolithic structure. These trends are characteristic of all the samples that were received.

The photon cross-correlation spectroscopy (PCCS) was used to determine the average particle size. According to particle size distribution curves of monofunctional samples presented in Fig. 3, the average diameter of particles of **Fe_3O_4@BM** is slightly smaller than of congruent **Fe_3O_4@BA** samples. In addition, for both types of samples, a tendency of narrowing particle size distribution with increasing content of functional groups was observed. Thus, the average diameters of **Fe_3O_4@BM4** and **Fe_3O_4@BA4** particles are about 181 and 195 nm, respectively. Different pictures were observed for bifunctional **Fe_3O_4@BAM** sample. While **Fe_3O_4@BAM8** particles are characterized by quite narrow particle size distribution with average diameter equal to 237 nm, the increase in the content of functional groups widens particle size distribution. In fact, the **Fe_3O_4@BAM4** sample contains four groups of agglomerates with maximum (in the range of decreasing intensity) of 575, 846, 342, and 1110 nm. It should be mentioned that according to our previous research conducted with polysilsesquioxane spherical particles with amino- (Stolyarchuk et al. 2016) and mercapto groups (Stolyarchuk et al. 2018), narrow distribution of particles in size is not typical for such materials. Such particles usually form agglomerates, which is facilitated by the presence of residual silanol groups on their surfaces. Incorporating magnetic core in the structure of the same particles, we could see (Fig. 3) that most of them have quite narrow size distributions, except for **Fe_3O_4@BAM4.** In this case, a large number of silanes contributed to the formation of agglomerates and their coalescence.

The IR spectroscopy was used to confirm the presence of the spatial network of siloxane bonds and functional groups in the samples that were synthesized. FTIR spectra are presented in Fig. 4. The presence of functional amino groups introduced during the synthesis of **Fe_3O_4@BA** (Fig. 4) is confirmed by two low-intensity absorption bands at 3305 and 3367 cm^{-1} in the IR spectra, referring to $\nu_{s,as}$ (N–H) stretches, as well as the medium intensity band at ca. 1590 cm^{-1} attributed to bending $\delta(NH_2)$. Meanwhile, mercapto groups in **Fe_3O_4@BM** samples (Fig. 4) possess the characteristic absorption band at 2576 cm^{-1}, which corresponds to ν_{as}(S–H) stretches. The same adsorption bands were used to confirm the functionalization of ceramic tubes with amino and mercapto functions using similar BTESE/APTES and BTESE/MPTMS systems (Tomina et al. 2017). Samples of magnetite with bifunctional surface layers,

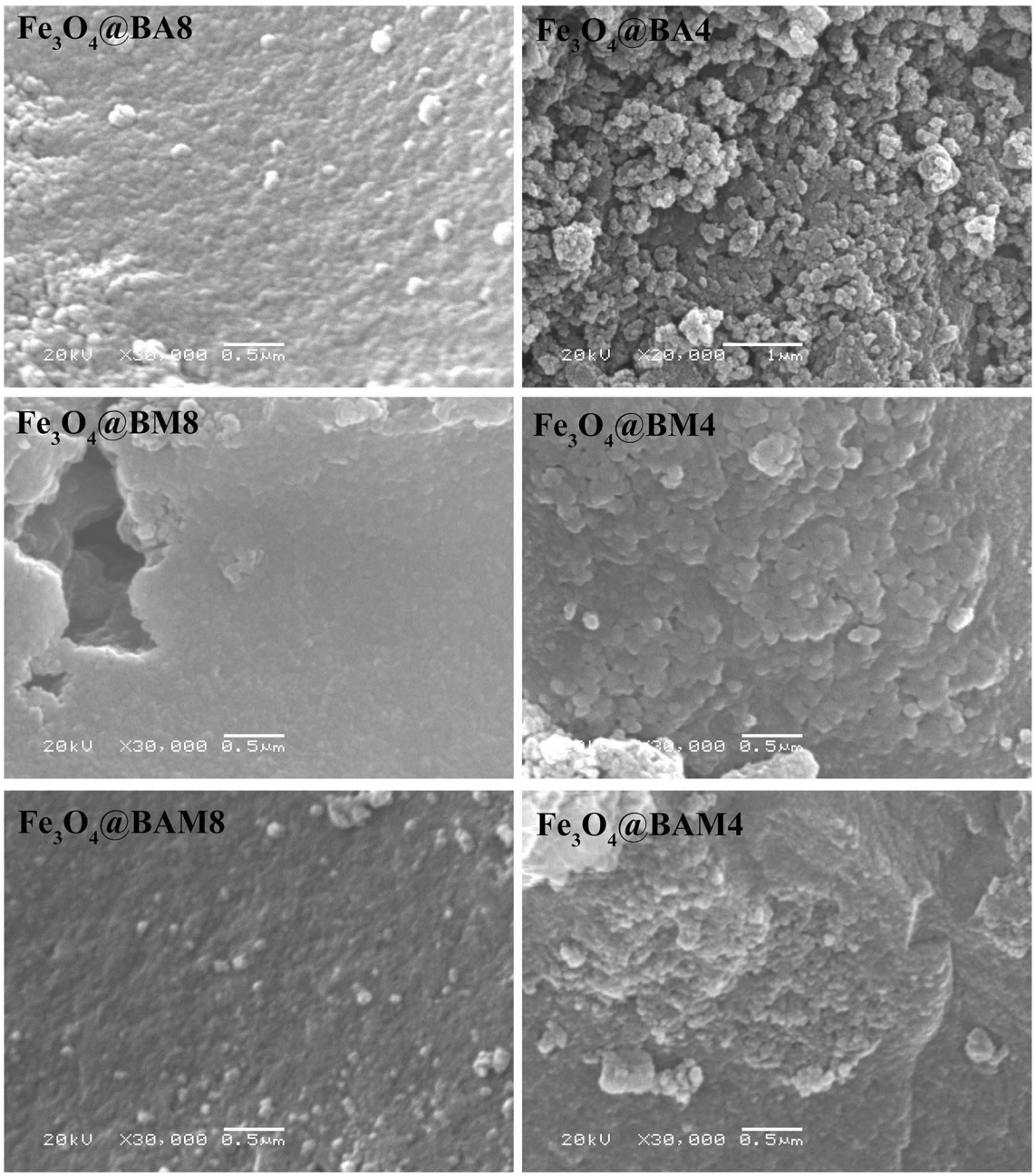

Fig. 2 SEM images of the composites of magnetite and mesoporous silica with amino- (**Fe_3O_4@BA4**, **Fe_3O_4@BA8**), mercapto- (**Fe_3O_4@BM4**, **Fe_3O_4@BM8**), and both types of groups (**Fe_3O_4@BAM4**, **Fe_3O_4@BAM8**) in the surface layer

Fe_3O_4@BAM (Fig. 4), contain characteristic absorption bands for both amino groups [ν_{as} (N–H) 3375, ν_s(N–H) 3303, δ(NH_2) 1589 cm^{-1}] and mercapto groups [ν_{as}(S–H) 2580 cm^{-1}].

The IR spectra of all samples possess a group of absorption bands in the region 2800–2980 cm^{-1} which correspond to the symmetric and asymmetric stretches of the C–H bonds in the propyl chain from the functional groups and the ethylene bridge of the bissilane. The presence of ethylene bridges between silicon atoms is also evidenced by two intense sharp absorption bands at ~ 1270 cm^{-1} and ~ 1415 cm^{-1}, which can be attributed to $\omega(CH_2)$ and $\delta(CH_2)$ of bridges ≡Si–CH_2–CH_2–Si≡ (Stolyarchuk et al. 2016). In addition, in the region of 1000–1200 cm^{-1}, the most intense broad absorption band due to ν(SiOSi) stretches is observed, indicating the presence of spatial polysiloxane network. The position of maximum of this band for the functionalized samples synthesized using TEOS is at about 1080 cm^{-1} (Tomina et al. 2017), whereas for polysilsesquioxane samples synthesized using BTESE, the band is shifted to lower

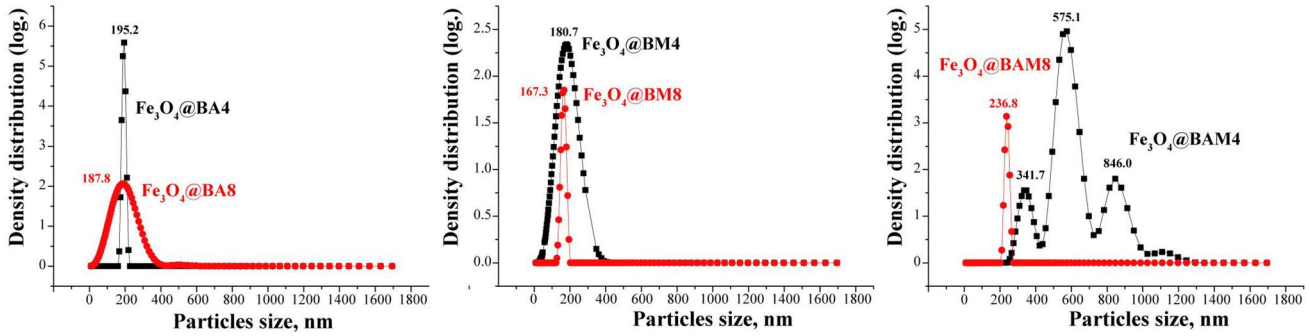

Fig. 3 Particles' size distribution

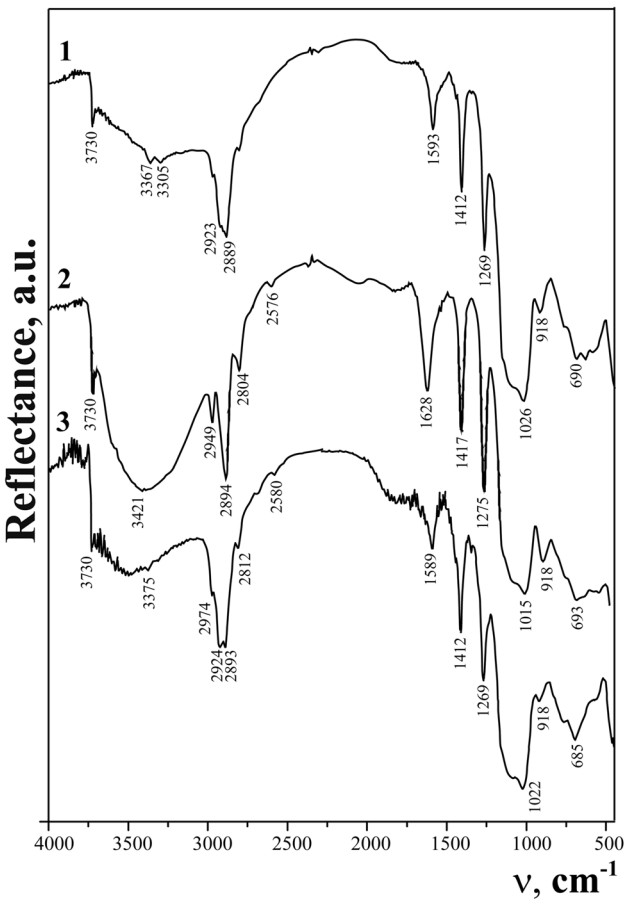

Fig. 4 IR spectra of the composites of magnetite and mesoporous silica with (1) amino propyl, (2) mercaptopropyl, and (3) both types of groups on the example of **Fe_3O_4@BA4**, **Fe_3O_4@BM4**, and **Fe_3O_4@BAM4** samples

frequencies (~ 1020 cm^{-1}) (Dabrowski et al. 2005; Tomina et al. 2017), similar to our case (Fig. 4).

All IR spectra of both pure Fe_3O_4 (Mel'nik et al. 2012) and functionalized contain an intense and wide absorption band of ν(FeO) in the region of 550–650 cm^{-1}. It also should be mentioned that all functionalized magnetite samples (Fig. 4) as well as the similar bridged particles (Stolyarchuk et al. 2016, 2018) and xerogels (Dabrowski et al. 2005) synthesized using BTESE have an absorption band at 3730 cm^{-1}, characteristic of stretching vibrations of silanol groups (McDonald 1958).

Consequently, according to the results of IR spectroscopy, it can be concluded that the obtained nanoparticles consist of iron oxide, a spatial network of siloxane bonds, bridges, functional groups introduced during synthesis by the corresponding functional silanes, and silanol groups.

Low-temperature isotherms of adsorption–desorption of nitrogen were recorded (Fig. 5) to determine the specific surface area, sorption volume, and pore diameter. The data calculated from adsorption–desorption isotherms are summarized in Table 1.

According to Yurchenko et al. (2013), the pH of the environment created by functional group affects the formation of the porous structure of polysilsesquioxane adsorbents. The strongly alkaline environment created by 3-aminopropyl groups promotes the formation of systems with type IV adsorption isotherms [according to IUPAC classification Sing et al. (1985)]. Meanwhile, thiol groups create neutral (or nearly neutral) environment providing for the formation of porous systems with Langmuir-type isotherms. In our case, such mechanism was clearly observed for **Fe_3O_4@BA4** and **Fe_3O_4@BM8** samples with amino and thiol groups, respectively (Fig. 5), whereas the isotherms of samples containing both amino and mercapto groups, **Fe_3O_4@BAM**, can be classified as a combination of I and IV types.

The isotherm of **Fe_3O_4@BA8** can be attributed to the combination of Types I and IV. It also should be mentioned that isotherms of both samples with amino groups have hysteresis loops of H2 type, witnessing the presence of mesoporous silica layer around the magnetic core. However, the average diameter of these mesopores is different. An increase of the portion of APTES in the reaction solution increased d_{aver} of pores from 3.7 to 9.5 nm (see samples **Fe_3O_4@BA8** and **Fe_3O_4@BA4** in Table 1);

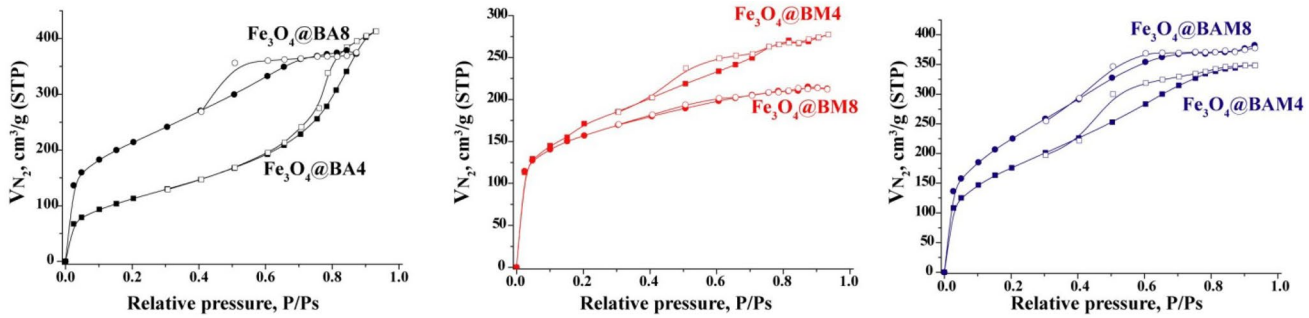

Fig. 5 Low-temperature nitrogen adsorption–desorption isotherms

however, it decreased the adsorption pore volume (from 0.7 to 0.64 cm^3/g) and specific surface area (from 750 to 408 m^2/g).

Contrary to the typical Langmuir-type isotherm of **Fe_3O_4@BM8** sample, the isotherm of **Fe_3O_4@BM4** sample with higher content of MPTMS can be attributed to the combined isotherm of Types I and IV (Fig. 5). Moreover, the type H2 hysteresis loop is obvious, which indicates the mesoporosity (d_{aver} = 3.7 nm, Table 1). The increase in the content of mercapto component leads to slight increase in the specific surface (from 520 to 575 m^2/g) and adsorption pore volume (from 0.33 to 0.43 cm^3/g).

As it was mentioned earlier, the isotherms of samples containing both amino and mercapto groups, **Fe_3O_4@BAM**, can be classified as I + IV type isotherms with H2-type hysteresis loops, indicating the mesoporosity. Herewith, the increase in the content of amino-component (APTES) in the reaction mixture increases the mesoporosity of the sample. The specific surface area of bifunctional samples is higher than those of monofunctional ones produced at the same structuring agent/functionalizing silanes ratio.

Thus, taking into account data from the low-temperature nitrogen adsorption–desorption isotherms' analysis, the functionalized magnetic particles that were synthesized are covered with polysilsesquioxane shells with well-developed porous structure. This structure is created using BTESE as a structure-forming agent.

Analysing the XRD data, it could be concluded that the size of crystallites in the initial magnetite is 11.8 nm; meanwhile, the core of the functionalized samples retains the structure of the initial magnetite. Functionalization of magnetite leads to the increase in the size of individual particles which was calculated using Debye–Scherrer's equation (Table 1). The samples with amino groups **Fe_3O_4@BA** are formed by the largest particles (due to the impact of amino groups from APTES on hydrolytic polycondensation observed earlier). Accordingly, the samples with mercapto groups **Fe_3O_4@BM** possess smaller sizes. It also should be mentioned that bigger quantity of BTESE contributes to the formation of larger shell of polysilsesquioxane coatings around magnetite. However, for bifunctional **Fe_3O_4@BAM,** there is no direct dependence between the particle size and the specific surface area, which is more affected by the structure development.

Adsorption properties of the samples were tested for silver(I), copper(II), and lead(II) ions (Fig. 6).

Compared to the non-functionalized sample of magnetite (Giraldo et al. 2013), magnetite–silica composites with surface functional groups (introduced using MPTMS and APTES) showed improved adsorption properties to heavy metal ions (see Table 2). An explanation for such an improvement is the interaction of metal ions with functional groups fixed in the surface layer. It is also known

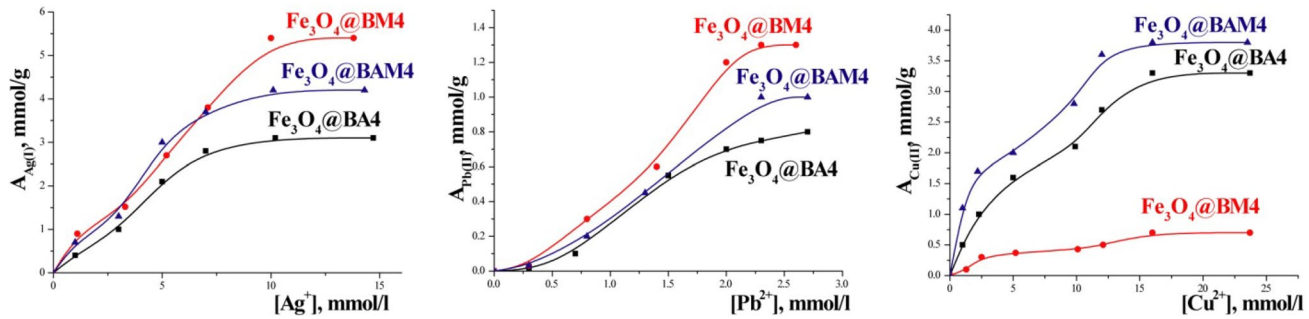

Fig. 6 Adsorption isotherms of some metal ions

Table 2 Comparative characteristic of the magnetite/silica composites with amine- and mercapto-functions

Sample	S_{sp} (m^2/g)	Cf. gr. (mmol/g)	SSC (mmol/g)			References
			(Cu^{2+})	(Pb^{2+})	(Ag^{+})	
Fe_3O_4	95.5	0	0.17	0.18	–	Giraldo et al. (2013)
Fe_3O_4@SiO_2–NH_2 [$Fe_3O_4/SiO_2/\equiv Si(CH_2)_3NH_2$]	216.2	1.6	0.47	0.37	–	Wang et al. (2010)
A [$Fe_3O_4/SiO_2/\equiv Si(CH_2)_3NH_2$]	122	2.2	0.42	–	0.3	Melnyk et al. (2016), Gdula et al. (2017)
AM [$Fe_3O_4/SiO_2/\equiv Si(CH_2)_3NH_2/\equiv SiCH_3$]	29	1.6	0.30	–	–	Melnyk et al. (2016)
NH_2–MNP [$Fe_3O_4/SiO_2/\equiv Si(CH_2)_3NH_2$]	–	–	0.39	–	–	Li et al. (2013)
Fe_3O_4@SBA-15-NH_2 [$Fe_3O_4/SiO_2/\equiv Si(CH_2)_3NH_2$]	344.3	2.02	–	0.72	–	Wang et al. (2015)
Fe_3O_4@BA4 [$Fe_3O_4/\equiv Si(CH_2)_2Si\equiv/\equiv Si(CH_2)_3NH_2$]	408	2.82	3.28	0.8	3.03	Current paper
S1 [$Fe_3O_4/SiO_2/\equiv Si(CH_2)_3SH$]	33	0.8	–	0.4	0.16	Melnyk et al. (2018)
SM1 [$Fe_3O_4/SiO_2/\equiv Si(CH_2)_3SH/\equiv SiCH_3$]	360	1.8	–	0.8	0.68	Melnyk et al. (2018)
Fe_3O_4@BM4 [$Fe_3O_4/\equiv Si(CH_2)_2Si\equiv/\equiv Si(CH_2)_3SH$]	575	0.93	0.70	1.3	5.40	Current paper
Fe_3O_4@BAM4 [$Fe_3O_4/\equiv Si(CH_2)_2Si\equiv/\equiv Si(CH_2)_3NH_2/\equiv Si(CH_2)_3SH$]	631	0.7 + 1.0	3.80	1.0	4.19	Current paper
Fe_3O_4@SiO_2@NH_2@SH [$Fe_3O_4/SiO_2/\equiv Si(CH_2)_3NH_2/\equiv Si(CH_2)_3SH$]	–	3.5 + 0.4	–	0.12	–	Izanloo et al. (2019)

that the amount of adsorption depends on the number of functional groups, their location, and spatial availability.

According to literature sources (Liu et al. 2008), amino-containing ligands have higher binding capability for copper(II) ions than, for example, for lead(II) ions. Therefore, it is not a surprise that among the tested cations, the sorption capacity of **Fe_3O_4@BA4** sample decreased in a range $Cu^{2+} > Ag^{+} > Pb^{2+}$. Mercapto group is known to possess strong affinity to various heavy metal ions (Hg^{2+}, Ag^{+}, Pb^{2+}, etc.) due to Lewis acid–base interactions (Vieira et al. 1997). Thus, in terms of decreasing adsorption capacity of **Fe_3O_4@BM4**, the tested cations can be arranged as follows: $Ag^{+} > Pb^{2+} > Cu^{2+}$. These results are consistent with those obtained for magnetite functionalized with mesoporous coating containing mercapto groups using template synthesis (Li et al. 2011). As for the sample with bifunctional surface layer, **Fe_3O_4@BAM4**, the highest uptake is observed for Ag^{+} presumably due to slightly higher content of mercapto groups. The second in rank are Cu^{2+} due to strong affinity to amino groups, while Pb^{2+} occupy the last place.

In general, all three tested samples are characterized by high uptake of Ag^{+}, Pb^{2+}, and Cu^{2+} (Fig. 6, Table 2). The highest values of static adsorption capacity towards silver(I) and lead(II) ions were observed for **Fe_3O_4@BM4** (5.4 and 1.3 mmol/g, respectively). The adsorption capacity values of the bifunctional composite, **Fe_3O_4@BAM4**, to silver(I) and lead(II) ions were 4.19 and 1.0 mmol/g, respectively. Meanwhile, the lowest sorption capacity was shown by magnetite composite with amino groups, **Fe_3O_4@BA4**, 3.03 and 0.8 mmol/g, respectively.

In the case of adsorption of copper(II) ions (Fig. 6), the highest static sorption capacity 3.8 mmol/g (247 mg/g) is characteristic for **Fe_3O_4@BAM4** sample. The **Fe_3O_4@BA4** sample has shown a sorption capacity of 3.28 mmol/g (214 mg/g). The lowest sorption capacity 0.7 mmol/g (46 mg/g) was found for the sample **Fe_3O_4@BM4**.

The zeta-potential measurements were performed before and after adsorption of metal ions to describe the interactions of metal ions with the surface groups of adsorbents. Various pH values of the initial metal ions solutions were chosen [pH (Ag^{+}) ~ 2.0, pH (Pb^{2+}) ~ 4.2, and pH (Cu^{2+}) ~ 5.0] and the differences were recorded. Due to partial protonation of amino groups, **Fe_3O_4@BA4** is characterized by highly positive values of zeta potential in the range of pH values 2–9, and its isoelectric point pI = 10 (Fig. 7). The sample with mercapto groups, **Fe_3O_4@BM4**, is characterized by negative values of zeta potential in the range of tested pH values due to weak acidic properties of thiol groups. The zeta potential of bifunctional sample **Fe_3O_4@BAM4** shows low positive values and is 'intermediate' between pure amino and pure mercapto samples. Its isoelectric point (pI = 7.5, Fig. 7) is shifted to lower pH value, compared to **Fe_3O_4@BA4**. This explains strong tendency of particles **Fe_3O_4@BAM4** to aggregation, witnessed during PCCS analysis (Fig. 3). Similar tendency in the ζ-potential values was described by Wani et al. 2012 for the mesoporous silica with mercapto (− 15 mV), amino (15.6 mV) and mercapto/amino groups (5.2 mV). It should also be mentioned that samples synthesized using bissilanes contain high quantities of silanol groups, the presence of which is confirmed by IR spectra recorded for the obtained samples (Fig. 4). These silanol groups could intensify a negative charge for the samples with negative surface and reduce positive charge for positive surface.

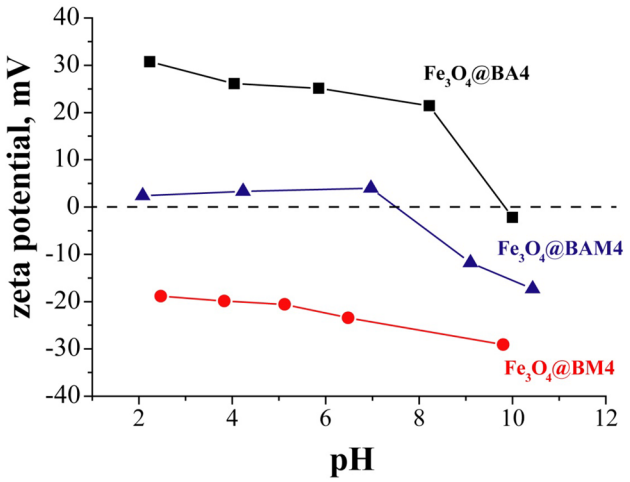

Fig. 7 ζ-potential curves for the composites of magnetite and mesoporous silica with amino **Fe_3O_4@BA4**, mercapto **Fe_3O_4@BM4**, and (3) both types of groups **Fe_3O_4@BAM4**

As it can be concluded from Table 3, during the adsorption of metal ions on **Fe_3O_4@BM4**, its negative ζ-potential value decreases in magnitude due to the interaction with cations $\mathbf{Fe_3O_4@S^- + Me^{n+} \rightarrow Fe_3O_4@(S)_nMe}$ and/or $\mathbf{Fe_3O_4@O^- + Me^{n+} \rightarrow Fe_3O_4@(O)_nMe,}$ although the electrostatic interaction (physical sorption) is also likely. Thus, despite higher adsorption capacity of Ag(I) ions, Cu(II) and Pb(II) ions have stronger effect on zeta potential; due to their valence 2, they can interact with 2 surface groups.

Regarding the adsorption of metal ions on the samples with amino groups, the adsorptive mechanism appears to be different. One of the mechanisms of adsorption of all the three tested cations on the **Fe_3O_4@BA4** is specific adsorption (a kind of chemisorption), since the positive surface charge became less positive at the addition of cations. Another interaction occurs due to metal–amine complexation. However, according to Li et al. 2013, analysing adsorption behavior of Cu(II) ions on amino-functionalized magnetic nanoparticles (Li et al. 2013), surface complexation mechanism is combined with ion exchange between amino groups and Me^{n+}. It should also be mentioned that electrokinetic potential is a very complicated phenomenon (Bhattacharjee 2016) that may depend on many factors (such as pH, ionic strength, valency of the ions, concentration, types of interactions on the surface, etc.). In case of **Fe_3O_4@BA4** adsorbent, the probability of solid–solid particle spontaneous coalescence is a very high due to the near zero surface charge; hence, the probability of simply entrapment of cations is also high (Bokányi et al. 2016).

Therefore, it is difficult to identify the key factor affecting the change in zeta potential of studied composites. According to the measurements presented in Table 3, the change in the zeta-potential values indicates the adsorption of metal ions on the surface. In addition, we can conclude that there are different mechanisms of adsorption on the obtained adsorbents. That is why, the adsorbed amounts vary from adsorbent to adsorbent and from cation to cation.

The affinity of synthetized composites towards organic dyes was examined as well. The screening adsorption tests were performed with Acid Red 88 and Methylene Blue (Fig. 8).

The interaction of composites with metal ions, high content, and accessibility of functional groups plays a key role in terms of adsorption of larger molecules such as organic dyes. Thus, for Acid Red 88 that has negatively charged sulfonate groups, the most effective adsorbents were samples **Fe_3O_4@BA4** (118 mg/g) and **Fe_3O_4@BAM4** (113 mg/g) which are characterized by positive zeta-potential values (Table 1). On the other hand, Methylene Blue with N-containing groups that can be protonated is easier to interact with negatively charged **Fe_3O_4@BM4** (−27.03 mV (Table 1). Consequently, the uptake of Methylene Blue was 88 mg/g by **Fe_3O_4@BM4**, 74 mg/g by **Fe_3O_4@BAM4**, 62 mg/g by **Fe_3O_4@BA4**, and these results correlate with the surface charges of the adsorbents (Table 1).

Conclusions

Three types of composites with a magnetite nucleus and a shell of mesoporous silica with 3-aminopropyl, 3-mercaptopropyl groups, and both 3-aminopropyl and

Table 3 The ζ-potential data of composites before and after adsorption of metal ions

Sample	Ag^+				Pb^{2+}				Cu^{2+}			
	Zp_1	Zp_2	Δ	A (mmol/g)	Zp_1	Zp_2	Δ	A (mmol/g)	Zp_1	Zp_2	Δ	A (mmol/g)
Fe_3O_4@BM4	−18.9	−7.1	11.8	5.4	−20.0	−4.3	15.8	1.3	−20.6	−3.3	17.3	0.7
Fe_3O_4@BA4	30.7	15.2	15.5	3.0	26.1	4.8	21.3	0.8	25.1	10.7	14.4	3.3
Fe_3O_4@BAM4	2.4	−1.3	3.7	4.2	3.3	−2.7	6.0	1.0	3.4	2.1	1.3	3.8

Zp_1—initial value of zeta potential at working pH, mV

Zp_2—zeta potential of the sample with adsorbed metal ions, mV

Δ—difference between Zp_1 and Zp_2

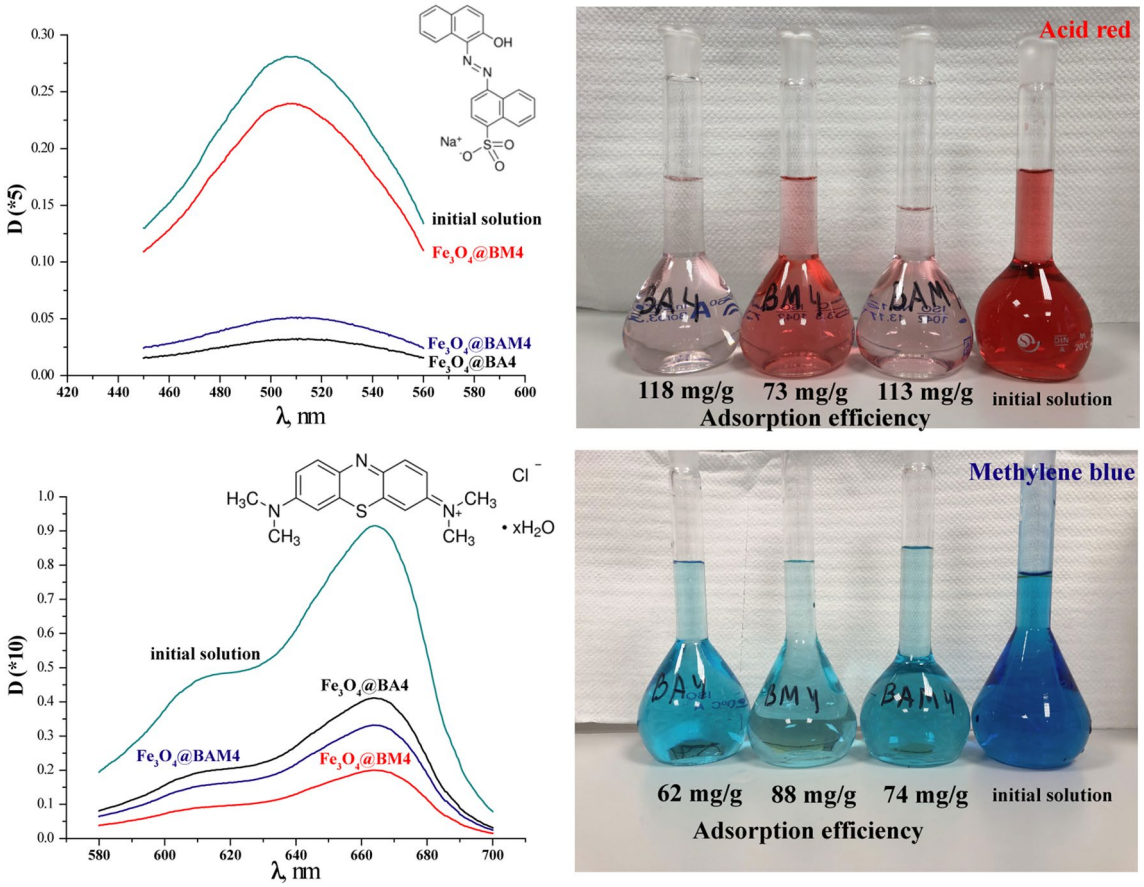

Fig. 8 Dyes adsorption study by the composites of magnetite and mesoporous silica with amino **Fe_3O_4@BA4**, mercapto **Fe_3O_4@BM4**, and (3) both types of groups **Fe_3O_4@BAM4**

3-mercaptopropyl groups were synthetized. According to the results of physical and chemical analyses, the obtained magnetic composites consist of 11.8 nm magnetite core coated with polysilsesquioxane layer bearing −SH and $-NH_2$ functional groups (elem. anal., IR). The size of composite particles reaches 20–30 nm (XRD). These primary particles form agglomerates about 200 nm (PCCS, SEM) with a specific surface area of 408–818 m^2/g. In general, the nature of the functional group affects the size of formed particles, their specific surface area, and ζ-potential values. Amino group, which contributes to the formation of alkaline medium, accelerates the sol–gel process resulting in the formation of larger particles with high specific surface area and creates a positive charge on the surface of the composites. However, composites with 3-mercaptopropyl groups possess negative surface charge, smaller particle sizes, and almost identical surface areas, regardless of the amount of the structuring agent. The bifunctional materials have all characteristics of amino-containing materials, but contain mercapto groups as well.

The maximum sorption capacities towards Ag(I), Pb(II), and Cu(II) ions during adsorption from aqueous solutions were shown to be 3.8, 1.3, and 5.4 mmol/g, respectively. At the same time, these composites can adsorb Acid Red 88 and Methylene Blue dyes up to 118 mg/g and 88 mg/g depending on the surface charge. Thus, the synthesized functionalized magnetite composites can be used as effective solid-phase extractants.

Acknowledgements The research was supported by the SASPRO Project No. 1298/03/01 of the FP7-PEOPLE-2013-COFUND-609427 Programme, the joint Ukrainian-Slovak research Project within the SAV-NASU cooperation and Project VEGA 2/0156/19 of the Scientific Grant Agency of the MŠVVaŠ SR.

Compliance with ethical standards

Conflict of interest The authors declare that they have no conflict of interest.

References

Bhattacharjee S (2016) DLS and zeta potential—what they are and what they are not? J Controlled Release 235:337–351. https://doi.org/10.1016/j.jconrel.2016.06.017

Bokányi L, Szabó S, Paulovics J (2016) Investigation of surface properties and floatability of CdTe semiconductor for the sake of recycling of obsolete solar elements. In: IMPC 2016—28th international mineral processing congress, Quebec, Canada: Canadian Institute of Mining, Metallurgy and Petroleum, Paper Code 135047, vol 5, pp 2917–2925. ISBN: 978-192687229-2

Chung J, Chun J, Lee J, Lee SH, Lee YJ, Hong SW (2012) Sorption of Pb(II) and Cu(II) onto multi-amine grafted mesoporous silica embedded with nano-magnetite: effects of steric factors. J Hazard Mater 239–240:183–191. https://doi.org/10.1016/j.jhazmat.2012.08.063

Dabrowski A, Barczak M, Stolyarchuk NV, Melnyk IV, Zub YL (2005) Bridged polysilsesquioxane xerogels functionalizated by amine- and thiol-groups: synthesis, structure, adsorption properties. Adsorption 11:501–517. https://doi.org/10.1007/s10450-005-5609-0

Dong J, Xu JZ, Wang F (2008) Engineering and characterization of mesoporous silica-coated magnetic particles for mercury removal from industrial effluents. Appl Surf Sci 254:3522–3530. https://doi.org/10.1016/j.apsusc.2007.11.048

Gdula K, Skwarek E, Dabrowski A, Melnyk I (2017) Amine-functionalized silica particles with magnetic core as magnetically removable adsorbents of Ag(I) ions. Adsorpt Sci Technol 35(5–6):432–438. https://doi.org/10.1177/0263617417694365

Giraldo L, Erto A, Moreno-Piraján JC (2013) Magnetite nanoparticles for removal of heavy metals from aqueous solutions: synthesis and characterization. Adsorption 19:465–474. https://doi.org/10.1007/s10450-012-9468-1

Goncharuk VV, Radovenchyk VM, Gomelya MD (2003) Obtaining and use of highly dispersed sorbents with magnetic properties. Shepetivska International Printing House, Kyiv, Ukraine

Hakami O, Zhang Y, Banks CJ (2012) Thiol-functionalised mesoporous silica-coated magnetite nanoparticles for high efficiency removal and recovery of Hg from water. Water Res 46(12):3913–3922. https://doi.org/10.1016/j.watres.2012.04.032

Huang C, Hu B (2008) Silica-coated magnetic nanoparticles modified with γ-mercaptopropyltrimethoxysilane for fast and selective solid phase extraction of trace amounts of Cd, Cu, Hg, and Pb in environmental and biological samples prior to their determination by inductively coupled plasma mass spectrometry. Spectrochim Acta, Part B 63:437–444. https://doi.org/10.1016/j.sab.2007.12.010

Izanloo M, Esrafili A, Jafari AJ, Farzadkia M, Behbahani M, Sobhi HR (2019) Application of a novel bi-functional nanoadsorbent for the simultaneous removal of inorganic and organic compounds: equilibrium, kinetic and thermodynamic studies. J Mol Liq 273:543–550. https://doi.org/10.1016/j.molliq.2018.10.013

Kim Y, Lee B, Yi J (2003) Preparation of functionalized mesostructured silica containing magnetite (MSM) for the removal of copper ions in aqueous solutions and its magnetic separation. Sep Sci Technol 38(11):2533–2548. https://doi.org/10.1081/SS-120022286

Kusyak NV, Kaminskiy OM, Petranovska AL, Gorbyk PP (2011) Adsorption of heavy metal cations on the surface of nanosized magnetite. Surface 3(18):151–155 **(in Ukrainian)**

Li G, Zhao Z, Liu J, Jiang G (2011) Effective heavy metal removal from aqueous systems by thiol functionalized magnetic mesoporous silica. J Hazard Mater 192:277–283. https://doi.org/10.1016/j.jhazmat.2011.05.015

Li H, Xiao D, He H, Lin R, Zuo P (2013) Adsorption behavior and adsorption mechanism of Cu(II) ions on amino-functionalized magnetic nanoparticles. Trans Nonferr Metals Soc China 23(9):2657–2665. https://doi.org/10.1016/s1003-6326(13)62782-x

Liu C, Bai R, San Ly Q (2008) Selective removal of copper and lead ions by diethylenetriamine-functionalized adsorbent. Behav Mech Water Res 42:1511–1522. https://doi.org/10.1016/j.watres.2007.10.031

McDonald RS (1958) Surface functionality of amorphous silica by infrared spectroscopy. J Phys Chem 62(10):1168–1178. https://doi.org/10.1021/j150568a004

Mel'nik IV, Zub YL, Alonso B, Abramov NV, Gorbik PP (2012) Creation of a functional polysiloxane layer on the surface of magnetic nanoparticles using the sol–gel method. Glass Phys Chem 38(1):96–104. https://doi.org/10.1134/S1087659611060113

Melnyk IV, Zub YL (2012) Preparation and characterisation of magnetic nanoparticles with bifunctional surface layer ≡ $Si(CH_2)_3NH_2$/≡ $SiCH_3$ (or ≡ SiC_3H_7–n). Microporous Mesoporous Mater 154:196–199. https://doi.org/10.1016/j.micromeso.2011.11.012

Melnyk IV, Gdula K, Dąbrowski A, Zub YL (2016) Magneto-sensitive adsorbents modified by functional nitrogen-containing groups. Nanoscale Res Lett 11:61. https://doi.org/10.1186/s11671-016-1273-4

Melnyk IV, Pogorilyi RP, Zub YL, Vaclavikova M, Gdula K, Dąbrowski A, Seisenbaeva GA, Kessler VG (2018) Protection of thiol groups on the surface of magnetic adsorbents and their application for wastewater treatment. Sci Rep 8:8592. https://doi.org/10.1038/s41598-018-26767-w

Ozmen M, Can K, Arslan G, Tor A, Cengeloglu Y, Ersoz M (2010) Adsorption of Cu(II) from aqueous solution by using modified Fe_3O_4 magnetic nanoparticles. Desalination 254:162–169. https://doi.org/10.1016/j.desal.2009.11.043

Pogorilyi RP, Melnyk IV, Zub YL, Seisenbaeva GA, Kessler VG, Shcherbatyik MM, Košak A, Lobnik A (2013) Urease adsorption and activity on magnetite nanoparticles functionalized with monofunctional and bifunctional surface layers. J Sol-Gel Sci Technol 68(3):447–454. https://doi.org/10.1007/s10971-013-2991-z

Pogorilyi RP, Melnyk IV, Zub YL, Seisenbaeva GA, Kessler VG (2014a) Immobilization of urease on magnetic nanoparticles coated by polysiloxane layers bearing thiol- or thiol- and alkyl-functions. J Mater Chem B 2:2694–2702. https://doi.org/10.1039/C4TB00018H

Pogorilyi RP, Melnyk IV, Zub YL, Seisenbaeva GA, Kessler VG (2014b) New product from old reaction: uniform magnetite nanoparticles from iron-mediated synthesis of alkali iodides and their protection from leaching in acidic media. RSC Adv 4(43):22606–22612. https://doi.org/10.1039/C4RA02217C

Sing KSW, Everett DH, Haul RAW, Moscou L, Pierotti RA, Rouquérol J, Siemieniewska T (1985) Reporting physisorption data for gas/solid systems with special reference to the determination of surface area and porosity (recommendations 1984). Pure Appl Chem 57(4):603–619. https://doi.org/10.1351/pac198557040603

Stolyarchuk NV, Barczak M, Melnyk IV, Zub YL (2016) Amine-functionalized nanospheres, synthesized using 1,2-bis(triethoxysilyl) ethane. In: Fesenko O, Yatsenko L (eds) Nanophysics, nanophotonics, surface studies, and applications. Springer proceedings in physics, vol 183. Springer, Cham, pp 415–425. https://doi.org/10.1007/978-3-319-30737-4_35

Stolyarchuk NV, Kolev H, Kanuchova M, Keller R, Vaclavikova M, Melnyk IV (2018) Synthesis and sorption properties of bridged polysilsesquioxane microparticles containing 3-mercaptopropyl groups in the surface layer. Colloids Surf A Physicochem Eng Asp 538:694–702. https://doi.org/10.1016/j.colsurfa.2017.11.049

Tan Y, Chen M, Hao Y (2012) High efficient removal of Pb(II) by amino-functionalized Fe_3O_4 magnetic nano-particles. Chem Eng J 191:104–111. https://doi.org/10.1016/j.cej.2012.02.075

Tang Y, Liang S, Wang J, Yu S, Wang Y (2013) Amino-functionalized core-shell magnetic mesoporous composite microspheres for Pb(II) and Cd(II) removal. J Environ Sci 25(4):830–837. https://doi.org/10.1016/S1001-0742(12)60141-7

Thanh NTK (2012) Magnetic nanoparticles: from fabrication to clinical applications. CRC Press, Boca Raton. ISBN: 9781439869321

Tomina VV, Stolyarchuk NV, Melnyk IV, Zub YL, Kouznetsova TF, Prozorovich VG, Ivanets AI (2017) Composite sorbents based on porous ceramic substrate and hybrid amino- and mercapto-silica materials for Ni(II) and Pb(II) ions removal. Sep Purif Technol 175:391–398. https://doi.org/10.1016/j.seppur.2016.11.040

Trofimchuk AK, Kuzovenko VA, Mel'nik IV, Zub YL (2006) Comparison of the complexation abilities of bifunctional polysiloxane xerogels and chemically modified silica gels. Russ J Appl Chem 79(2):229–235. https://doi.org/10.1134/S1070427206020121

Turanska SP, Kaminsky AN, Kusjak NV, Turov VV, Gorbyk PP (2012) Synthesis, properties and application of magnetodirected adsorbents. Surface 4(19):266–292 **(in Russian)**

Vieira EFS, JdeA Simoni, Airoldi C (1997) Interaction of cations with SH-modified silica gel: thermochemical study through calorimetric titration and direct extent of reaction determination. J Mater Chem 7(11):2249–2252. https://doi.org/10.1039/A704286H

Wang J, Zheng S, Shao Y, Liu J, Xu Z, Zhu D (2010) Amino-functionalized Fe_3O_4@SiO_2 core–shell magnetic nanomaterial as a novel adsorbent for aqueous heavy metals removal. J Colloid Interface Sci 349:293–299. https://doi.org/10.1016/j.jcis.2010.05.010

Wang S, Wang K, Dai C, Shi H, Li J (2015) Adsorption of Pb2 + on amino-functionalized core–shell magnetic mesoporous SBA-15 silica composite. Chem Eng J 262:897–903. https://doi.org/10.1016/j.cej.2014.10.035

Wani A, Muthuswamy E, Savithra Layan GH, Mao G, Brock S, Oupický D (2012) Surface functionalization of mesoporous silica nanoparticles controls loading and release behavior of mitoxantrone. Pharm Res 29(9):2407–2418. https://doi.org/10.1007/s11095-012-0766-9

Xin X, Wei Q, Yang J, Yan L, Feng R, Chen G, Du B, Li H (2012) Highly efficient removal of heavy metal ions by amine-functionalized mesoporous Fe_3O_4 nanoparticles. Chem Eng J 184:132–140. https://doi.org/10.1016/j.cej.2012.01.016

Yurchenko GR, Matkovskii AK, Stolyarchuk NV, Mel'nik IV, Zub YL (2013) Adsorption properties of bridged polysilylsesquioxane xerogels functionalized with amino, mercapto, and phosphonic groups. Prot Metals Phys Chem Surf 49(4):392–397. https://doi.org/10.1134/S2070205113040163

Zavoiura O, Zaporozhets O, Volovenko O, Melnyk IV, Zub YL (2015) Silica-coated magnetite nanoparticles modified with 3-aminopropyl groups for solid phase extraction of Pd(II) ions from water solutions. Adsorpt Sci Technol 33(3):297–306. https://doi.org/10.1260/0263-6174.33.3.297

Zhang Z, Zhang F, Zhu Q, Zhao W, Ma B, Ding Y (2011) Magnetically separable polyoxometalate catalyst for the oxidation of dibenzothiophene with H_2O_2. J Colloid Interface Sci 360:189–194. https://doi.org/10.1016/j.jcis.2011.04.045

Zhang S, Zhang Y, Liu J, Xu Q, Xiao H, Wang X, Xu H, Zhou J (2013) Thiol modified Fe_3O_4@SiO_2 as a robust, high effective, and recycling magnetic sorbent for mercury removal. Chem Eng J 226:30–38. https://doi.org/10.1016/j.cej.2013.04.060

Zub YL, Melnyk IV, Stolyarchuk NV, Dobryans'ka HI, Barczak M, Dabrowski A (2005) Comparative characteristics of texture and properties of hybrid organic–inorganic adsorbents functionalized by amine and thiol groups. Prog Solid State Chem 33:179–186. https://doi.org/10.1016/j.progsolidstchem.2005.11.028

Zub YL, Melnyk IV, White MG, Alonso B (2008) Structural features of surface layers of bifunctional polysiloxane xerogels containing 3-aminopropyl groups and 3-mercaptopropyl groups. Adsorpt Sci Technol 26:119–133. https://doi.org/10.1260/026361708786035440